Proceedings of the Sixth International Conference on
Railway Technology: Research, Development and Maintenance
Edited by: J. Pombo
Civil-Comp Conferences, Volume 7, Paper 9.3
Civil-Comp Press, Edinburgh, United Kingdom, 2024
ISSN: 2753-3239, doi: 10.4203/ccc.7.9.3

Dynamics-Based Estimation of Wheel-Rail Friction Coefficient using Deep CNN

B. Abduraxman[1], P. Hubbard[1], T. Harrison[1], C. Ward[2], D. Fletcher[3], R. Lewis[3], K. Chandrasekhar[4] and D. Vincent[4]

[1]Wolfson School of Mechanical, Electrical and Manufacturing Engineering, Loughborough University, United Kingdom
[2]Rail Accident Investigation Board, Derby, United Kingdom
[3]The Department of Mechanical Engineering, The University of Sheffield, United Kingdom
[4]Hitachi Rail, London, United Kingdom

Abstract

This paper presents an estimation scheme for rail-wheel friction coefficients applying a multi-channel deep convolutional neural network on axlebox accelerations. Different to conventional approaches, the multi-channel deep convolutional neural network does not depend on any slip or creep measurements, nor knowledge of vehicle parameters. It is trained using axlebox longitudinal and lateral acceleration measurements and known rail friction coefficient measurements obtained from running a rail vehicle on friction-modified tracks with five different friction levels at four different speeds. The experimental test data includes both straight and curved track scenarios, and independent validation data shows that the friction coefficient can be very accurately estimated under normal running conditions in almost all of the validation data sets.

Keywords: friction coefficient estimation, low adhesion detection, wheel-rail friction, convolutional neural networks, railway, condition monitoring.

1 Introduction

Insufficient rail-wheel friction occurs due to contaminations present within the wheel-

rail interface such as wet-rail or compressed leaves, resulting in poor adhesion conditions that leads to critical safety and operational issues. To mitigate the risk of wheel spin/slide, global solutions such as the widespread uptake of defensive driving are required that result in network wide disruption for potentially localised issues [1]. Poor adhesion conditions are costly to the network and also presents a barrier to increasing capacity due to their impact on stopping the trains with reliability and predictability under various adhesion conditions [2]. These problems show the importance of knowing accurate adhesion levels so that adverse effects are minimized [3].

The friction coefficient can be similarly defined as the adhesion/traction coefficient μ_a, which is commonly defined as the ratio between the reactive tangential force from the rail to wheel F_c and wheelset load Q. Maximum μ_a is usually equal to maximum kinetic friction coefficient μ [4], which gives:

$$\mu_{amax} = \frac{F_{cmax}}{Q} \approx \frac{F_{fmax}}{N} = \mu \tag{1}$$

where μ_{amax} and F_{cmax} are the maxima of μ_a and F_c, and F_{fmax} is the maximum kinetic friction. In general, estimation of μ can directly provide the estimation of maximum adhesion coefficient μ_{amax} in many contact models [6], and μ_{amax} is the crucial safety limiting value that is relevant to a wheel slip or slide.

The friction coefficient depends on a number of factors due to the complex and nonlinear interaction between the rail and the wheel, including wheel-rail geometries and track irregularities [7], weather conditions [8], surface roughness, and contact surface temperature [9]. These factors make adhesion estimation a challenging and complex task [5].

Adhesion/friction estimations can also be achieved by estimations of the contact/creep forces, or slip/creepage curves based on some contact or adhesion models [5][6]. Kalman filters (KFs), Kalman-Bucy filters (KBFs) are also popular in adhesion estimation research. KBFs were used in [10]-[16] to estimate the creep/contact forces, and these forces were used to estimate the adhesion levels in [10]-[12]. estimation of Examples of unscented KFs (UKFs) used for adhesion estimation are given in [17]-[18]. The authors in [19] used a joint-UKF for a friction coefficient estimator, however, it requires at least 10 seconds of incoming data to reasonably estimate step changes in friction levels. Multi-body physics simulation tools can also be used to generate vehicle responses for adhesion estimation [20].

Applications of machine learning or artificial neural networks (ANNs) for rail friction/adhesion level estimations are very few. ANN was first used for adhesion estimation in [21], where a recurrent NN (RNN) provided a better estimation than a conventional method. A feedforward NN (FNN) was trained and validated in [22] with experimental measurements of vehicle speed, wheelset angular speed, and brake pressure to accurately estimate the adhesion levels. An FNN is also implemented in

[23] as part of a kernel extreme learning machine with radial basis function (RBF) and particle swarm optimization to estimate stable and unstable regions of adhesion. An FNN estimator was reported in [24] to show that the friction coefficient can be accurately estimated using only axlebox longitudinal accelerations and vehicle/wheelset speed. All of these estimators use shallow NNs (SNNs) with only a single hidden layer, which cannot extract higher level features. Compared to SNNs, DNNs provide the capability of higher level feature extraction for classification (or regression) [25]. Authors in [26] have designed a multi-layer perceptron (MLP) with two hidden layers on seven acoustic features in frequency domain extracted from rolling noise in a twin-disk machine for detecting dry and wet conditions at two different speeds. The friction coefficient estimation problem can be treated as the popular time series classification (TSC) problem. Convolutional neural networks (CNNs) are one of the most widely used architecture for TCS, owing to their temporal, and spatial-invariance, robustness and relatively shorter training time compared to RNNs or MLPs [25]. Nevertheless, there is only a single application of CNN in estimation of friction/adhesion coefficients given in [27], where friction coefficients for dry and wet conditions were accurately estimated from forward-facing camera and vertical railhead images.

Almost all of the adhesion estimations are based on the knowledge of slip, which can be subject to significant drift if any velocity term in the slip is obtained by time-integrating acceleration signals [24]. Therefore, based on the same idea of using only axlebox accelerations as in the previous work [24], a multichannel deep CNN (MC-DCNN) is applied to axlebox accelerations to accurately estimate the friction coefficient in this paper. Similarly, the MC-DCNN does not depend on slip/adhesion curve, creep force models, or braking commands as in [22]. To apply the convolution filters, the 1D time series wheelset accelerations are simply converted to 2D signals by stacking overlapping segments of past samples vertically to the current time samples. The wheelset acceleration and friction coefficients measurements data are from a series of field tests, where an instrumented full-size two-car test vehicle was driven on a friction-modified test track under five different friction levels at four different running speeds. The MC-DCNNs estimation performance is carried out using both longitudinal and lateral axlebox accelerations on straight and curved track runs. Independent validation data sets show that the network can accurately and consistently estimate the friction coefficients.

2 Method

This section explains the test data used, data processing and architecture of the MC-DCNN.

2.1 Test data

The test data used was obtained from a series of field tests carried out in an 800-m test track facility in Tuxford, where a fully instrumented 2-car multi-purpose vehicle (MPV) owned by Network Rail with a pair of four-wheel bogies were driven on the

friction-modified track. In addition to the default dry condition, four different friction conditions were created by applying industry standard railhead conditioning products. Three-axis accelerometers were custom-fit on left and right axleboxes of all four wheelsets to measure left and right wheel accelerations. Note that axlebox and wheel accelerations are assumed the same. All data was recorded via an onboard data acquisition system at a sampling rate of 5120 Hz. Other details of the test procedures and creation and measurement of different friction levels are provided in [24][28][29].

Compared to previous work [24], the data sets now constitutes all available test runs carried out at constant speeds for both straight and curved tracks. In addition, the validation data sets are selected from totally different test runs, instead of selecting different portions of the same test runs as in [24].

Speed	**16 mph**	**26 mph**	**40 mph**	**60 mph**
		Straight track		
Dry	0.31	0.29	0.31, 0.37	0.3,0.34,0.35
Friction modifier	0.14,0.17	0.19	0.17	0.16
Wet	0.161	0.19	0.24, 0.24	0.27
Detergent	0.18,0.17	0.21	0.17, 0.22	0.24
Paper tape	0.16,0.2	0.07,0.16,0.22	0.1	0.11, 0.19
		Curved track		
Dry	0.28	0.32	0.31	0.36
Friction modifier	0.13, 0.26	0.26	0.27	0.27
Wet	0.35, 0.23	0.19	0.25	-
Detergent	0.28	0.25, 0.28	0.28, 0.32	0.28

Table 1. Friction levels achieved on the test track for constant speed runs.

The friction measurements for all 50 test runs are tabulated in
Table 1. The orange coloured friction values represent validation data sets, and the rest of the data are used for training. The validation data sets are selected such that there is at least one training data for that speed and friction condition, except for the case of 60 mph Detergent on the curved track.

2.2 Data processing

All data has been downsampled by a factor of 10 to a sampling rate of 512 Hz. This was done to reduce both the training time and network size, and it had no effect on prediction accuracy. A high-pass filter (HPF) with 0.00005 Hz cut-off frequency is then applied, with the very low cut-off frequency removing substantial drift in the data that could lead to drifts in the estimations. The HPF also removes the DC offsets in the accelerometers. The HPF is followed by a low pass filter (LPF) with 1 Hz of cut-off frequency to remove high frequency signals that could otherwise lead to oscillations in the estimations.

The N-samples of filtered 1D acceleration signals are then converted into 2D signals by stacking a rolling past samples of 0.25 second window vertically at the

current samples, which produces N-by-128 dimensional data. Taking a window length longer than 0.25 seconds did not improve the estimation results.

The acceleration signals contain positive and negative amplitudes that are not necessarily equal. This can be due to the combination of overall vehicle condition, nonlinearities, keeper plate modes of vibration, conicity and any asymmetries in mass distribution and suspension parameters along each axis, leading to asymmetric oscillations. Asymmetric oscillations can also be skewed towards the direction of travel, and negatively dominant oscillations can become positively dominant when the train is travelling in the opposite direction. To reduce the effect of asymmetries and direction of travel, absolute norms are applied to the filtered accelerations, which has shown to be important for estimation accuracy.

2.3 Architecture

The MC-DCNN consists of 5 1D convolutional layers (CLs), denoted by CL1, CL2, CL3, CL4, and CL5, respectively, each CL followed by a ReLU layer and an average pooling layer (APL). The last APL is connected to a fully connected layer (FCL). The outputs of each CL are referred as feature vectors (FVs). The ReLU layer helps reduce overfitting, while the pooling layer reduces the dimensions of the FVs and the network size for faster training and implementation. For inputs, all four wheelset accelerations are used because, intuitively, all four wheelset behaviour can contribute to the knowledge of friction. Only longitudinal wheelset accelerations were used in [24], but here, both longitudinal and lateral wheelset accelerations are used for inputs. The architecture of the MC-DCNN is shown in Figure 1, where μ_{est} is the estimated friction coefficient, and the ReLU and pooling layers are not shown. Note that the inputs are also commonly normalized to [-1,1] for improved training.

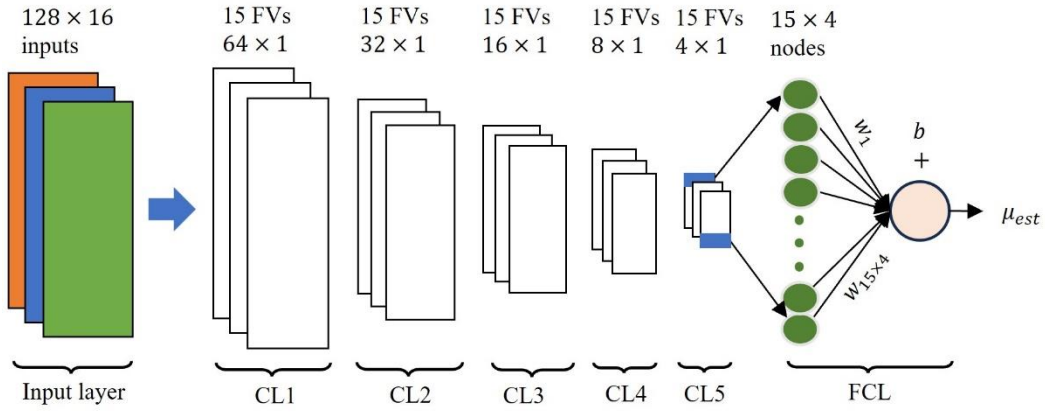

Figure 1: Architecture of the MC-DCNN.

The number of convolution filter heads chosen for all CLs is 15, with a filter length 3, a stride of 1, and same padding. The APLs have a size and stride of 2, resulting the input length of 128 to be halved after each APL. The FVs from the final pooling layer is flattened by the FCL, which then connects every element of the FVs to a single

neuron, as in an MLP. There are no activation functions in the FCL neurons; they just pass the flattened FV elements and multiplies them by a 1D weight matrix and adds a bias term to their weighted sum. This was because adding a sigmoid or tanh activation function did not improve the estimations.

In the multi-channel CNN, each convolutional filter head also has a number of channels of convolution filters that are equal to the number of channels in the previous layer. The number of FVs then determines the number of channels in subsequent convolutional layers. Thus, the actual number of convolution filters in CLs are 15-by-16, 15-by-15, 15-by-15, 15-by-15, and 15-by-15, respectively. This gives a number of learnable parameters for the network as 3555 including the bias terms.

The size and number of layers of the network was found to be sufficient for all speed cases after some training and validation studies. It was discovered that having more CLs improved the consistency of the estimations between different networks on the validation data. A single network is trained for both straight and curved track since there are much less test data for the curved track. In this way, the MC-DCNN can also learn common features between both straight and curved tracks, which helps its estimation performance on the curved track.

3 Results

To assess the estimation performance, we have recorded both the RMSE and mean absolute error (MAE) between the measured and estimated friction coefficients μ and μ_{est}. The network parameters are initialized randomly, and hence, to reduce the effect of random initialization on validation performance, 10 MC-DCNNs were repeatedly trained and validated for each speed case, and the average RMSEs, average MAE, and the standard deviation (SD) of MAEs from these 10 MC-DCNNs are tabulated in Table 2. The table also shows average of $\bar{\mu}_{est}$ from 10 MC-DCNNs, where $\bar{\mu}_{est}$is the mean from a single validation study.

Speed	**16 mph**	**26 mph**	**40 mph**	**60 mph**
Straight track				
Measured μ	0.17	0.16	0.17	0.34
Average $\bar{\mu}_{est}$	0.163	0.175	0.263	0.34
Average RMSE	0.0097	0.0181	0.0926	0.0082
Average MAE	0.0095	0.0178	0.0926	0.0081
SD (MAE)	0.0062	0.0128	0.0083	0.0065
Curved track				
Measured μ	0.13	0.25	0.32	0.28
Average $\bar{\mu}_{est}$	0.163	0.263	0.299	0.288
Average RMSE	0.0339	0.0199	0.0223	0.016
Average MAE	0.0334	0.0196	0.0223	0.0159
SD (MAE)	0.0113	0.0159	0.0206	0.0104

Table 2: The average $\bar{\mu}_{est}$, average RMSEs, average MAE, and SD of MAEs from 10 MC-DCNNs on validation data set.

Above table shows the MC-DCNN can estimate the friction coefficient accurately, except for the case of 40 mph Dry run. The very low SD of MAE means that the estimations between these 10 networks are also very consistent, suggesting robustness against random parameter initializations. To illustrate the network performance from a single validation study, typical estimation performances on the validation data for each speed cases are provided from Figure 2 to Figure 5, where the front and back sections of the plot show estimations on straight and curved tracks, respectively, that are concatenated to show on the same plot. These figures also show that the fluctuations in the estimations are small.

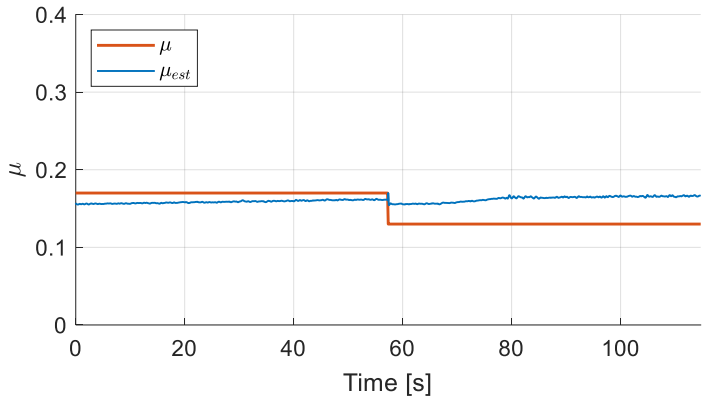

Figure 2. Estimation performance of an MC-DCNN at 16 mph. For straight track: RMSE=0.0114, MAE=0.0112. For curved track: RMSE=0.0328, MAE= 0.0326.

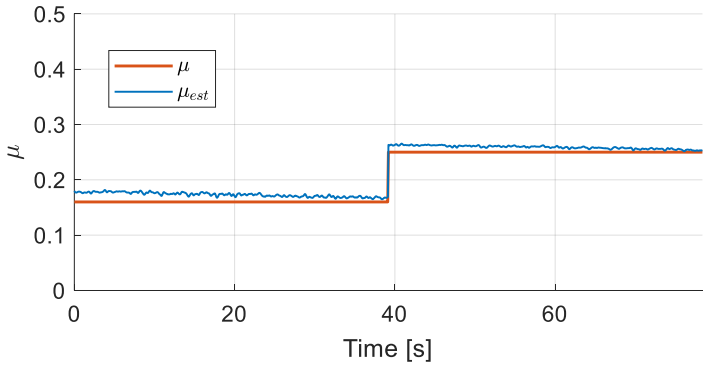

Figure 3. Estimation performance of an MC-DCNN at 26 mph. For straight track: RMSE=0.0138, MAE=0.0132. For curved track: RMSE=0.0094, MAE= 0.009.

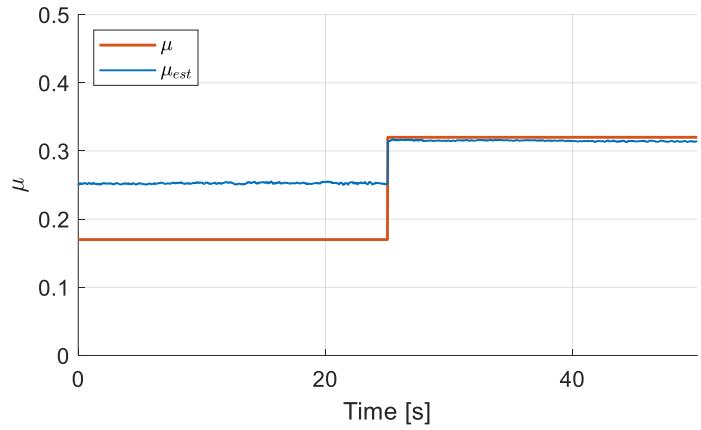

Figure 4. Estimation performance of an MC-CNN at 40 mph. For straight track: RMSE=0.0826, MAE=0.0826. For curved track: RMSE=0.0051, MAE= 0.0051.

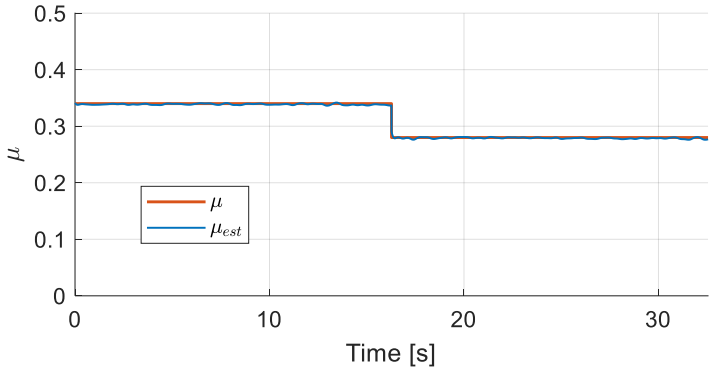

Figure 5. Estimation performance of an MC-CNN at 60 mph. For straight track: RMSE=0.0017, MAE=0.0014. For curved track: RMSE=0.0016, MAE= 0.0012.

The reason for poor estimation in the case of 40 mph Dry run can be due to the selection of the validation data set on this run. This is because it was found that the NN performance is slightly different for different validation data sets.

4 Conclusions

This paper has demonstrated that the various friction coefficients of a rail vehicle can be accurately estimated using MC-DCNN on axlebox accelerations only, with the knowledge wheelset/vehicle speed. The methodology does not depend on specific knowledge of creep/adhesion curves, or vehicle models, and is not subject to drift as in slip-based estimations. Future work entails investigating the performance of the method using different combinations of axlebox acceleration inputs and validation data set.

Acknowledgements

The authors would like thank Network Rail UK for financially sponsoring this project.

References

[1] Rowell B, Richardson W. An assessment of the available adhesion and slip risk for ERTMS. London: RSSB; 2003.

[2] RSSB, Adhesion. Accessed: 07/03/2023. Available at: https://www.rssb.co.uk/en/what-we-do/key-industry-topics/adhesion.

[3] Spiryagin, M, Cole C, Sun YQ, et al. General modelling techniques. Design and simulation of rail vehicles. Boca Raton, Florida: CRC Press/Taylor and Francis; 2014. p. 79–95.

[4] B. Chen, Z. Huang, W. Liu, R. Zhang, F. Zhou and J. Peng, "A Novel Adhesion Force Estimation for Railway Vehicles Using an Extended State Observer," *IECON 2019 - 45th Annual Conference of the IEEE Industrial Electronics Society*, Lisbon, Portugal, 2019, pp. 225-230, doi: 10.1109/IECON.2019.8926857.

[5] Sundar Shrestha, Qing Wu & Maksym Spiryagin (2019). Review of adhesion estimation approaches for rail vehicles, International Journal of Rail Transportation, 7:2, 79-102, DOI: 10.1080/23248378.2018.1513344.

[6] Sajjad Z. Meymand, Alexander Keylin & Mehdi Ahmadian (2016). A survey of wheel–rail contact models for rail vehicles, Vehicle System Dynamics, 54:3, 386-428, DOI: 10.1080/00423114.2015.1137956.

[7] Olofsson U, Lewis R. Tribology of the wheel- rail contact. In: Iwnicki S, editor. Handbook of railway vehicle dynamics. Boca Raton, FL: CRC Press; 2006. p. 121–138.

[8] Lyu Y, Bergseth E, Olofsson U. Open system tribology and influence of weather condition. Scientific Reports. 2016; 6:32455.

[9] Chen H, Tanimoto H. Experimental observation of temperature and surface roughness effects on wheel/rail adhesion in wet conditions. Int J Rail Transportation. 2018; 6:101–112.

[10] Ward CP, Goodall RM, Dixon R, et al. Adhesion estimation at the wheel–rail interface using advanced model-based filtering. Vehicle Syst Dyn. 2012; 50:1797–1816.

[11] Hubbard PD, Ward C, Dixon R, et al. Models for estimation of creep forces in the wheel/rail contact under varying adhesion levels. Vehicle Syst Dyn. 2014; 52:370–386.

[12] P.D. Hubbard, G.A. Amarantidis, C.P. Ward. (2016) Leaves on the Line: Low Adhesion Detection in Railways. *IFAC-PapersOnLine* 49:21, pages 467-472.

[13] Ward C, Goodall RM, Dixon R. Creep force estimation at the wheel-rail interface. 22nd International Symposium on Dynamics of Vehicles on Roads and Tracks; 2011 Aug, Manchester, UK. p. 1–6.

[14] Ward CP, Goodall RM, Dixon R. Contact Force Estimation in the Railway Vehicle Wheel Rail Interface. 18th International Federation of Automatic Control (IFAC); 2011 Jan, Milano, Italy. p. 4398–4403.

[15] Hubbard PD, Ward C, Dixon R, et al. Verification of model-based adhesion estimation in the wheel-rail interface. Chem Eng Trans. 2013; 33:757–762.

[16] Hubbard PD, Ward C, Goodall RM, et al. Real time detection of low adhesion in the wheel/rail contact. RRUKA Annual Conference; 2012, London, UK; p. 1–5.
[17] Zhao Y, Liang B, Iwnicki S. Friction coefficient estimation using an unscented Kalman filter. Vehicle Syst Dyn. 2014; 52:220–234.
[18] Yunshi Zhao, Longjiang Shen, Zhongcheng Jiang, Bo Zhang, Guoyun Liu, Yao Shu & Bo Peng (2023). Real-time wheel–rail friction coefficient estimation and its application, Vehicle System Dynamics, DOI: 10.1080/00423114.2022.2159846.
[19] Onat A, Voltr P, Lata M. A new friction condition identification approach for wheel–rail interface. Int J Rail Transportation. 2017; 5:127–144.
[20] Harrison, T., Hubbard, P.D., Ward, C.P., Goodall, R.M. Development of low adhesion estimation algorithms using data from wheelset and bogie mounted inertial sensors, 13th World Congress on Railway Research, Birmingham UK, 6-10 June 2022.
[21] Gajdar T, Rudas I, Suda Y. Neural network based estimation of friction coefficient of wheel and rail. IEEE International Conference on Intelligent Engineering Systems; 1997 Sep, Budapest, Hungary p. 315–318.
[22] Malvezzi M, Pugi L, Papini S, et al. Identification of a wheel–rail adhesion coefficient from experimental data during braking tests. Proceedings Institution Mechanical Engineers, Part F: Journal Rail Rapid Transit. 2013; 227:128–139.
[23] Jianhua Liu, Linfan Liu, Jing He, Changfan Zhang, Kaihui Zhao. Wheel/Rail Adhesion State Identification of Heavy-Haul Locomotive Based on Particle Swarm Optimization and Kernel Extreme Learning Machine. *Journal of Advanced Transportation* 2020, pages 1-6.
[24] Bilal Abduraxman, Peter Hubbard, Tim Harrison, Christopher Ward, David Fletcher, Roger Lewis & Ben White (2024). Acceleration-based friction coefficient estimation of a rail vehicle using feedforward NN: validation with track measurements, Veh. Sys. Dyn., DOI: 10.1080/00423114.2024.2323600.
[25] Ismail Fawaz, H., Forestier, G., Weber, J. *et al.* Deep learning for time series classification: a review. *Data Min. Knowl. Disc.* 33, 917–963 (2019). https://doi.org/10.1007/s10618-019-00619-1.
[26] Shrestha, Sundar & Koirala, Anand & Spiryagin, Maksym & Wu, Qing.. Wheel-Rail Interface Condition Estimation (W-RICE), 2020.
[27] Folorunso, M. O., Watson, M., Martin, A., Whittle, J. W., Sutherland, G., and Lewis, R. (May 12, 2023). "A Machine Learning Approach for Real-Time Wheel-Rail Interface Friction Estimation." ASME. *J. Tribol*. September 2023; 145(9): 091102. https://doi.org/10.1115/1.4062373.
[28] White B, Lewis R, Fletcher D, Harrison T, Hubbard P, Ward C. Rail-wheel friction quantification and its variability under lab and field trial conditions. *Proceedings of the Institution of Mechanical Engineers, Part F: Journal of Rail and Rapid Transit*. 2023; 0(0). doi:10.1177/09544097231209483.

[29] Harrison, T., Abduraxman, B., Hubbard, P., Ward, C., White, B., Fletcher, D., Lewis, R., Chandrashekar, K., Vincent, D., Chaney, S., Burstow, M., Cockroft, E., ‘Creation of and measurement of Low Adhesion Conditions for the development of on-train Low Adhesion Detection equipment’, International Association for Vehicle System Dynamics Symposium, Ottawa, Canada, August 2023.